

Alternative ball-milling synthesis of vanadium-substituted polyoxometalates as catalysts for the aerobic cleavage of C-C and C-O bonds

Louay Al-Hussaini ^{a,b}, S. Valange ^c, M.E. Gálvez ^{b,*} and F. Launay ^{a,*}

(a) Sorbonne Université, CNRS, UMR 7197, Laboratoire de Réactivité de Surface (LRS), F-75005 Paris, France

franck.launay@sorbonne-universite.fr

(b) Sorbonne Université, CNRS, UMR 7190, Institut Jean le Rond d'Alembert, F-75005 Paris, France

elena.galvez_parruca@sorbonne-universite.fr

(c) Institut de Chimie des Milieux et Matériaux de Poitiers (IC2MP), Université de Poitiers, CNRS, ENSI Poitiers, B1, 1 rue Marcel Doré, F-86073 Poitiers Cedex 9, France

CONTENT

1. Further information on the protocols and results of the elemental analysis	S2
Table S1. Weight engaged and elemental analyses (from ICP) of the different V_x prepared	S2
2. XRD profiles and Rietveld refinement (Case of V_3 materials)	S2
Figure S1. XRD profiles of V_3 -HT vs. JCPDS 00-043-0317 ($H_3PMo_{12}O_{40} \cdot 13H_2O$)	S2
Table S2. Refinement results of V_3 -HT and V_3 -BM ₅₀ -1 _{BM} -1.5 _{HT} vs. reference $H_3PMo_{12}O_{40} \cdot 13H_2O$	S2
3. TGA analysis (Principle for the determination of n / Case of V_x-BM₅₀-1_{BM}-1.5_{HT} materials)	S3
Figure S2. TGA-DSC profiles of V_x -BM ₅₀ -1 _{BM} -1.5 _{HT} catalysts vs V_3 -HT	S3
Table S3. Values of T_1 and T_2 for V_x -HT and V_x -BM ₅₀ -1 _{BM} -1.5 _{HT} materials measured by TGA	S4
4. Liquid ³¹P NMR (Principle of quantification)	S4
Table S4. Isomers proportions in $PMoV_2$ catalysts	S4
Figure S3. NMR profile of V_2 -BM ₅₀ -1 _{BM} -1.5 _{HT} , peaks of V_2 isomers	S5
5. Liquid ³¹P NMR (Case of V_2 materials)	S5
Figure S4. ³¹ P NMR spectra of V_2 -BM ₂₀ -1-1.5 _{HT} vs. V_2 -BM ₅₀ -1 _{BM} -1.5 _{HT} material in D_2O - H_2O 50-50	S5
6. XRD profiles (Case of V_2-BM₂₀-t_{BM}-t_{HT} materials)	S6
Figure S5. Influence of the milling (t _{BM}) and attack duration (t _{HT}) on XRD profiles of V_2 -BM ₂₀ -t _{BM} -t _{HT} materials vs. V_2 -BM ₅₀ -1 _{BM} -1.5 _{HT}	S6
7. Liquid ³¹P NMR (Case of V_2-BM₂₀-t_{BM}-t_{HT})	S6
Figure S6. ³¹ P NMR spectra of V_2 -BM ₂₀ -t _{BM} -t _{HT} and V_2 -BM ₅₀ -1 _{BM} -1.5 _{HT} materials in D_2O - H_2O 50-50	S6
8. TGA analysis (Case of V_2-BM₂₀-t_{BM}-t_{HT} materials)	S7
Figure S7. TGA-DSC profiles of V_2 -BM ₂₀ -t _{BM} -t _{HT} catalysts vs. V_2 -BM ₅₀ -1-1.5 _{HT} (V_2 -BM ₅₀ reference)	S7
9. Energy consumption: detailed calculation (HT vs BM)	S7
Table S5. Calculation of the energy consumption of V_3 -HT and V_x -BM ₅₀ -1 _{BM} -1.5 _{HT} synthesis procedures	S8
Table S6. Calculation of the energy consumption of V_2 -BM ₂₀ -t _{BM} -t _{HT} synthesis procedures	S8
10. XRD of ball-milled oxides	S9
Figure S8. XRD profiles of the mixed oxides ($x_{th} = 2$). (The (110) signal was used for Debye-Scherrer	S9

calculations)

Table S7. Crystallite size of BM mixed oxides vs. a hand mixture of oxides S9

11. Synthesis of K S9

12. HPLC analysis and calibration curves ($\lambda = 220$ nm) S10

Figure S9. Chromatogramm of the reaction mixture for **K1_{HT}** cleavage in the presence of V₃-BM₅₀-1_{BM}-1.5_{HT} S10

Figure S10. HPLC calibration curves of the products and reactants S11

13. References S11

1. Further information on the protocols and results of the elemental analysis

Table S1. Weight engaged and elemental analyses (from ICP) of the different V_x prepared

V _x		MoO ₃ (g)	V ₂ O ₅ (g)	H ₃ PO ₄ (g)	V (%wt.)	Mo (%wt.)	P (%wt.)
HT	V ₃ -HT	3.93	0.92	0.39 (85 wt.%)	7.06	46.2	2.01
BM ₅₀	V ₃ -BM ₅₀ -1 _{BM} -1.5 _{HT}	1.12	0.24	0.24 (28.5 wt.%)	8.02	49.9	1.80
	V ₂ -BM ₅₀ -1 _{BM} -1.5 _{HT}	1.21	0.15	0.26 (28.5 wt.%)	5.23	53.2	1.74
BM ₂₀	V ₂ -BM ₂₀ '-1 _{BM} -1.5 _{HT}				6.23	54.5	1.69
	V ₂ -BM ₂₀ -1 _{BM} -3 _{HT}			0.07 (85 wt.%) ^a	7.13	56.4	1.21
	V ₂ -BM ₂₀ -2 _{BM} -1.5 _{HT}	3.02	0.38	+ 0.04 g H ₂ O	5.82	53.7	1.67
	V ₂ -BM ₂₀ -2 _{BM} -3 _{HT}				7.03	56.3	1.51
	V ₂ -BM ₂₀ -4 _{BM} -1.5 _{HT}				6.96	55.8	1.33
	V ₂ -BM ₂₀ -4 _{BM} -3 _{HT}				7.01	56.0	1.38
	V ₂ -wBM ₅₀ -1-1.5 ^b	1.21	0.19	0.06 (85 wt.%) + 50 g H ₂ O	n. d.	n. d.	n. d.

^a 1.70 g of mixed oxide was used. ^b One-pot synthesis with the introduction of MoO₃, V₂O₅ and H₃PO₄ together.

2. XRD profiles and Rietveld refinement (Case of V₃ materials)

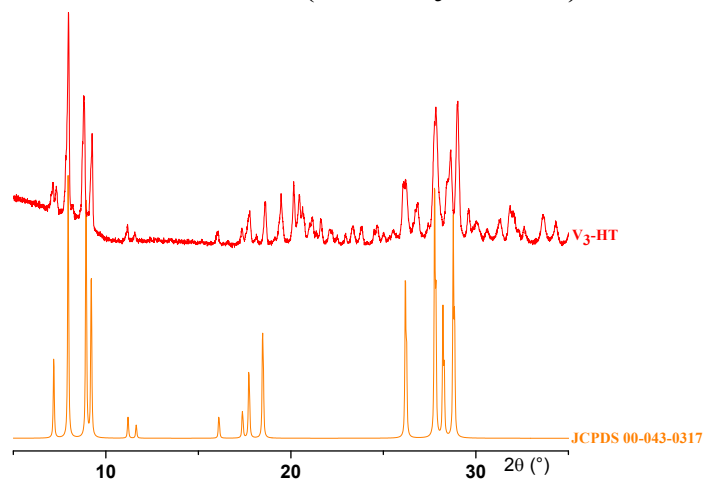


Figure S1. XRD profiles of V₃-HT vs. JCPDS 00-043-0317 (H₃PMo₁₂O₄₀. 13H₂O)
(Conditions detailed in the experimental section of the manuscript)

Table S2. Refinement results of V₃-HT and V₃-BM₅₀-1_{BM}-1.5_{HT} vs. reference H₃PMo₁₂O₄₀. 13H₂O

Sample	Cell parameters						R _p	Chi ₂
	a	b	c	α	β	γ		
V ₃ -BM ₅₀ -1 _{BM} -1.5 _{HT}	14.028	14.189	13.586	112.58	109.71	60.53	10	2.4
V ₃ -HT	14.219	14.410	13.616	112.54	110.13	60.13	15	13
Reference H ₃ PMo ₁₂ O ₄₀ . 13H ₂ O	14.100	14.130	13.550	112.10	109.80	60.70	-	-

3. TGA analysis (Principle for the determination of n / Case of V_x-BM materials)

The TGA profiles of V_x (H_{3+x}PMo_{12-x}V_xO₄₀, nH₂O) catalysts all exhibited two characteristic weight losses corresponding to n equivalents of hydration water (completed at T = T₁)^{R1} and to the loss of 0.5*(3+x) equivalents of constitutional water (for T₁ < T < T₂)^{R2}.

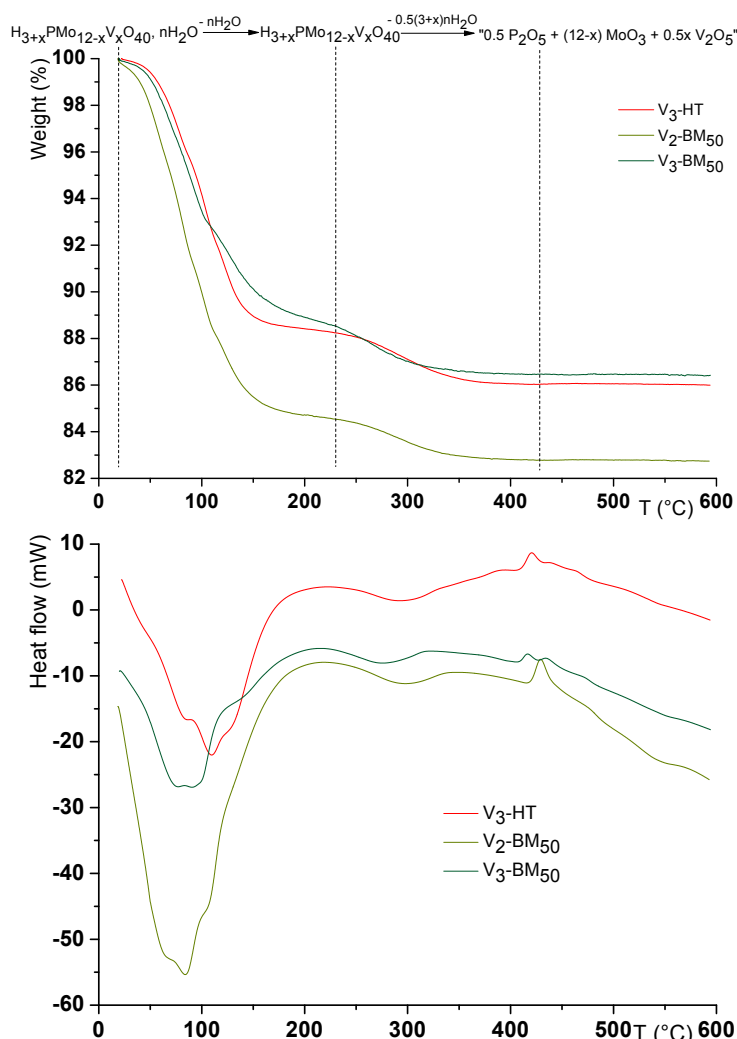


Figure S2. TGA-DSC profiles of V_x-BM₅₀-1_{BM}-1.5_{HT} (V_x-BM₅₀) catalysts vs V₃-HT
(Conditions detailed in the experimental section of the manuscript)

Even if x_{exp} can be calculated by TGA-DSC, ICP was preferred because, especially for V₃, the evaporation of hydration and of constitutive water are overlapped^{R3}. The equation used for x_{exp} calculation is:

$$x_{exp} = \frac{12}{1 + \frac{M_V w_{Mo}}{M_{Mo} w_V}}$$

where w_{Mo} and w_V are the weight proportions of Mo and V.

The hydration index n can be obtained from the first weight loss, $\Delta m_1\%$, since it is related to n

as follows:

$$\Delta m_1\% = 100M_{H_2O} \frac{n}{M_{V_x}} = 100M_{H_2O} \frac{n}{M_{V_{x,d}} + nM_{H_2O}}$$

where $V_{x,d}$ corresponds to the dehydrated form of V_x . $M_{V_{x,d}}$, the molecular weight of $V_{x,d}$ can be obtained by :

$$M_{V_{x,d}} = M_{PMo_{12}} - 43.992x$$

where PMo_{12} is the phosphomolybdic acid ($H_3PMo_{12}O_{40}$).

Table S3. Values of T_1 and T_2 for V_x -HT and V_x -BM₅₀-1_{BM}-1.5_{HT} materials measured by TGA

x_{th}	r	t_{BM} (h)	t_{HT} (h)	Name	T_1 (°C)	T_2 (°C)
3	-	0	6.5	V_3 -HT	222.1	420.6
2	50	1	1.5	V_2 -BM ₅₀ -1 _{BM} -1.5 _{HT}	218.7	429.1
3		1	1.5	V_3 -BM ₅₀ -1 _{BM} -1.5 _{HT}	215.8	416.4
2	20	1	1.5	V_2 -BM ₂₀ '-1 _{BM} -1.5 _{HT}	222.6	428.4
			3	V_2 -BM ₂₀ -1 _{BM} -3 _{HT}	214.7	428.4
		2	1.5	V_2 -BM ₂₀ -2 _{BM} -1.5 _{HT}	232.9	430.9
			3	V_2 -BM ₂₀ -2 _{BM} -3 _{HT}	214.0	428.3
		4	1.5	V_2 -BM ₂₀ -4 _{BM} -1.5 _{HT}	213.7	428.0
			3	V_2 -BM ₂₀ -4 _{BM} -3 _{HT}	211.2	427.4





4. Liquid ³¹P NMR (Principle of quantification)

In the conditions used, the ³¹P NMR integration of the signals is quantitative (see details and hypotheses the manuscript). The yield of V_x (η_{V_x}) was calculated as shown below:

$$\eta_{V_x} = 100 \frac{I_{V_x}}{I_{V_x} + I_{H_3PO_4}}$$

where I_{V_x} and $I_{H_3PO_4}$ are the integrations of V_x and of unreacted H_3PO_4 signals.

Table S4. Isomers proportions in PMoV₂ catalysts

Isomer ^a					
Chemical shift (ppm) ^b	-4.21	-4.03	-3.94	-3.77	
Localization of V atoms	Vicinal on the same triad	Vicinal on different triads	Not vicinal	n. d.	
Proportions (%)	V_2 -BM ₅₀ -1 _{BM} -1.5 _{HT}	58.5	12.6	16.3	12.7
	V_2 -BM ₂₀ '-1 _{BM} -1.5 _{HT}	47.9	17.1	24.0	11.0
	V_2 -BM ₂₀ -1 _{BM} -3 _{HT}	42.2	18.7	27.0	12.1
	V_2 -BM ₂₀ -2 _{BM} -1.5 _{HT}	49.1	14.3	23.3	13.3
	V_2 -BM ₂₀ -2 _{BM} -3 _{HT}	46.0	19.1	20.6	14.2
	V_2 -BM ₂₀ -4 _{BM} -1.5 _{HT}	45.2	14.7	25.5	14.6

$V_2\text{-BM}_{20}\text{-4BM-3}_{HT}$	37.4	23.8	21.1	17.7
PMoV ₂ 30 mg in H ₂ O-D ₂ O 1:1 500 μ L + 7.5 μ L dioxane, 400 MHz, 16 scans, relaxation delay: 32 s; n. d. = not defined				
^a α and β -isomer structures were taken from Refs R4 and R5 (β -4,10 and β -4,11 are two examples of β isomer), ^b See Fig. S3.				

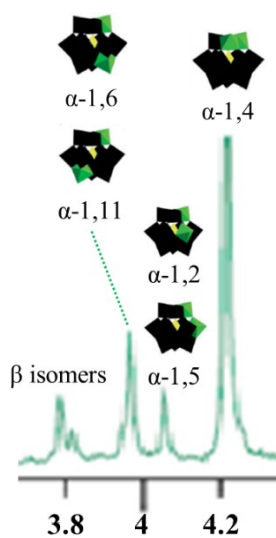


Figure S3. NMR profile of $V_2\text{-BM}_{50}\text{-1BM-1.5}_{HT}$, peaks of V_2 isomers

5. Liquid ³¹P NMR (Case of V_2 materials)

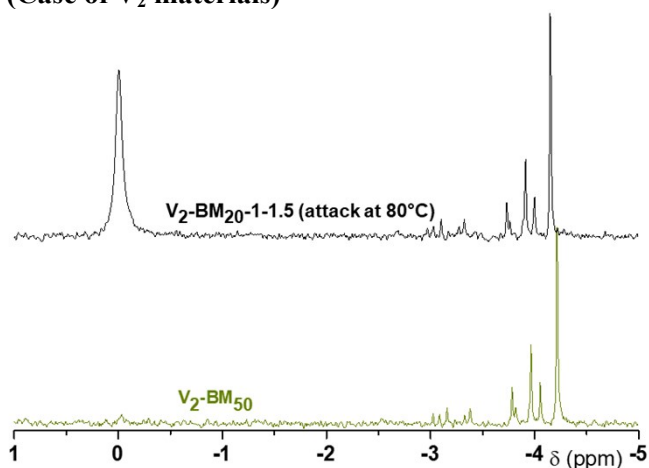


Figure S4. ³¹P NMR spectra of $V_2\text{-BM}_{20}\text{-1-1.5}_{HT}$ vs. $V_2\text{-BM}_{50}\text{-1-1.5}_{HT}$ ($V_2\text{-BM}_{50}$) material in D₂O-H₂O 50-50

6. XRD profiles (Case of $V_2-BM_{20}-t_{BM}-t_{HT}$ materials)

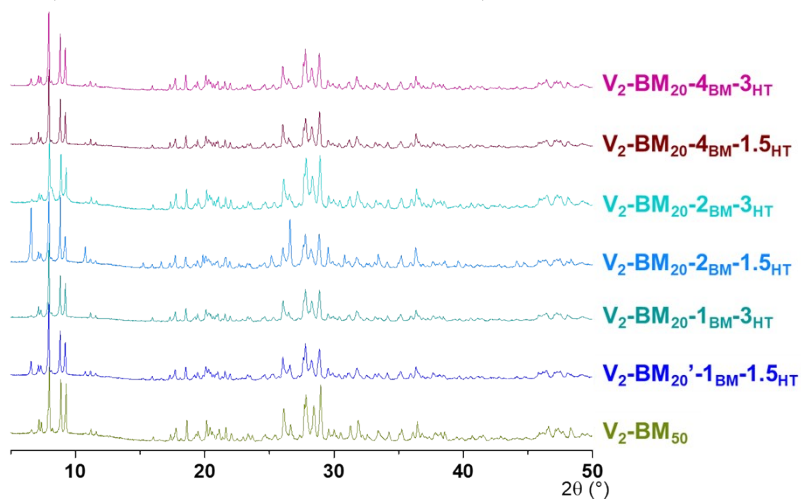


Figure S5. Influence of the milling (t_{BM}) and attack duration (t_{HT}) on XRD profiles of $V_2-BM_{20}-t_{BM}-t_{HT}$ materials vs. $V_2-BM_{50}-1-1.5_{HT}$ (V_2-BM_{50})

7. Liquid ^{31}P NMR (Case of $V_2-BM_{20}-t_{BM}-t_{HT}$)

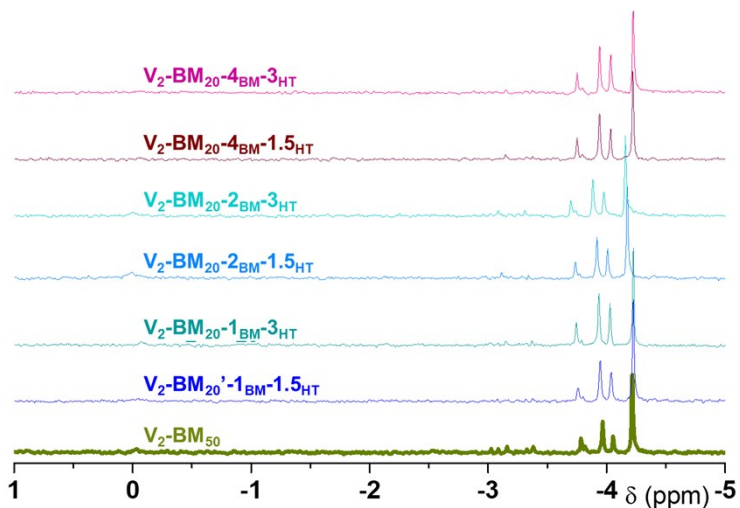


Figure S6. ^{31}P NMR spectra of $V_2-BM_{20}-t_{BM}-t_{HT}$ materials vs. $V_2-BM_{50}-1-1.5_{HT}$ (V_2-BM_{50}) in D_2O-H_2O 50-50

8. TGA analysis (Case of $V_2BM_{20-t_{BM}-t_{HT}}$ materials)

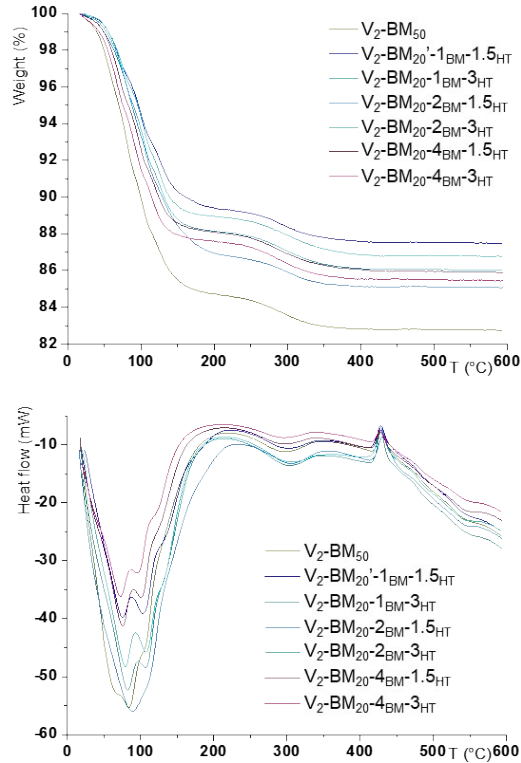


Figure S7. TGA-DSC profiles of $V_2-BM_{20-t_{BM}-t_{HT}}$ materials vs. $V_2-BM_{50-1-1.5_{HT}}$ (V_2-BM_{50} reference)

9. Energy consumption: detailed calculation (HT vs BM)

The electric power required for the electronic device is much lower than the required power for the milling and the attack steps. So, it can be neglected. Therefore, the equation of the global energy consumption is:

$$E_{tot} = E_{BM} + E_{HT} + E_c = P_{BM}t_{BM} + P_{HT}t_{HT} + P_c t_c$$

where E_{BM} , E_{HT} and E_c are respectively the contribution of the milling, of the attack steps and of the cooling systems to the total energy consumption.

The power required for the reflux condenser (noted P_c) during the attack was estimated using the Bernoulli equation:

$$\rho g z = \frac{P_c}{Q}$$

where $\rho = 10^3 \text{ kg m}^{-3}$, $g = 9.81 \text{ m s}^{-2}$, $z = 20 \text{ cm}$ (height of the condenser), $Q \approx 150 \text{ L/h}$

In these conditions: $P_c = 8.4 \cdot 10^{-2} \text{ W}$.

The maximal power of the heater used is $P_{th,max} = 825 \text{ W}$ and the maximal temperature noted T_{max} is 300°C . Supposing the starting temperature is 20°C , as the energy is proportional to the

rise of the temperature, the average power noted P_{HT} required for the thermal heating until a

$$P_{HT} = \left(\frac{T - 20}{T_{max} - 20} \right) P_{max}$$

temperature T is given by the equation:

$$\text{For } T = 100^\circ\text{C}, P_{HT} = 236 \text{ W} \Rightarrow P_c \ll P_{HT} \text{ and therefore, for } V_{HT} \text{ solids, } E_t \approx P_{BM}t_{HT}$$

In the case of V_{BM} materials, the ball-milling step (with a range of rotation speed, $100 < \omega < 1100$ rpm) has also to be considered. The maximal power (for $\omega_{max} = 1100$ rpm) is $P_{BM,max} = 1100$ W. As the combined weight of the sample and of the ball represent less than 10% of the autoclave, it can be asserted that it almost does not have any influence on the energy consumption. Therefore, the power needed for the milling procedure is proportional to the square of the rotation speed of the autoclave^{R6} and can be calculated by the formula:

$$P_{BM} = \left(\frac{\omega}{\omega_{max}} \right)^2 P_{BM,max}$$

Also, the power required for the cooling system (P_c') can be estimated to 5-20 W^{R6}. So, likewise the hydrothermal procedure, $P_c + P_c' \ll P_{BM} + P_{HT}$ and $E_t \approx P_{BM}t_{HT} + P_{BM}t_{HT}$

The values for the energy consumption required by the preparation of all the materials prepared are given in Tables S6 (V_3 -HT and V_x -BM₅₀) and S7 (V_2 -BM₂₀).

Table S5. Calculation of the energy consumption of V_3 -HT and V_x -BM₅₀-1_{BM}-1.5_{HT} synthesis procedures

Procedure (temperature)	Hydrothermal (100°C)	Ball milling, r = 50 (80°C)	
x_{th}	3	2	3
Milling duration (h)	0		1
Energy consumption during the milling step (kW.h)	0		0.45
Attack duration (h)	6.5		1.5
Energy consumption by heating (kW.h)	1.53		0.27
Global energy consumption (kW.h)	1.53		0.72
Weight (g)	5.345	2.897	2.937
Yield (%)	79	97	95
Global energy consumption (kW.h mol⁻¹)	627	437	431

Table S6. Calculation of the energy consumption of V_2 -BM₂₀-t_{BM}-t_{HT} synthesis procedures

Procedure	Ball-milling, r = 20					
Milling duration (h)	1	1	2	2	4	4
Energy consumption during the milling step (kW.h)	0.45	0.45	0.89	0.89	1.78	1.78
Attack duration (h)	1.5	3	1.5	3	1.5	3
Temperature (°C)	100	80	80	80	80	80
Energy consumption by heating (kW.h)	0.35	0.53	0.27	0.53	0.27	0.53
Global energy consumption (kW.h)	0.80	0.98	1.16	1.52	2.05	2.31
Global energy consumption (kW.h mol⁻¹)	198	240	287	357	508	563

Maximum anhydrous P_{Mo}V_x 6.950 g, yield 92-97%

10. XRD of ball-milled oxides

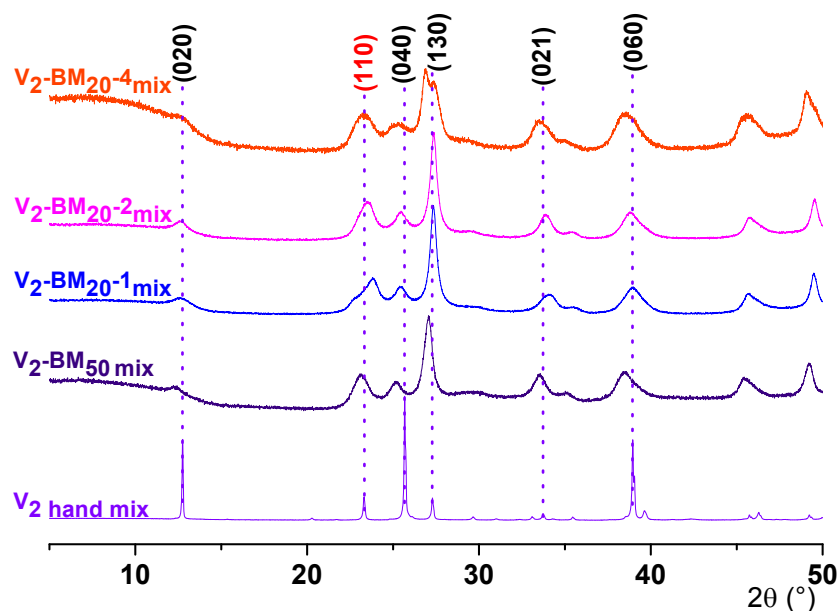


Figure S8. XRD profiles of the mixed oxides ($x_{th} = 2$). (The (110) signal was used for Debye-Scherrer calculations)

Herein, the aim is to compare the crystallite size of the mixtures before and after milling and we do not seek to calculate them accurately. So, the Scherrer equation will be used:

$$\tau = \frac{K\lambda_{Cu}}{L_{FWHM} \cos^2(\theta)}$$

where $K = 0.888$ is the shape factor, $\lambda_{Cu} = 1.5408 \text{ \AA}$ is the X-Ray wavelength, L_{FWHM} is the full width at half maximum of the considered peak (here (110)) and 2θ is the position of the peak.

Table S7. Crystallite size of BM mixed oxides vs. a hand mixture of oxides

Entry	Oxide	r	t_{BM} (h)	L_{FWHM} (°)	Position of the peak (110) (°)	Crystallite size (Å)
1	V_2 hand mix	-	-	0.1434	23.31	15.6
2	V_2 -BM ₅₀	50	1	0.9486	23.08	2.8
3	V_2 -BM ₂₀₋₁ mix	20	1	1.4469	23.49	1.4
4	V_2 -BM ₂₀₋₂ mix	20	2	1.3897	23.80	1.3
5	V_2 -BM ₂₀₋₄ mix	20	4	1.1693	23.49	1.7

11. Synthesis of K

The procedure was inspired by NICHOLS *et al*^{R7}. Hence, 2-bromoacetophenone (16.85 g, 84 mmol) and an excess of phenol (9.56 g, 101 mmol) were dissolved in 200 mL of acetone, then 20 g of K₂CO₃ were added to the solution. The mixture may take a pink coloration due to the formation of phenolate that disappears with time. Reflux is needed during 6 h to get **K**. Initially pale yellow, the coloration became yellow and then orange. The reaction was monitored by TLC using cyclohexane/diethylether 80/20 as the eluent. After filtration and acetone evaporation, **K** was recrystallized in a minimum amount of absolute ethanol. **K** was then recovered by filtration and dried by pressing. The formation of the ether bond was checked by FT-IR by the presence of a band at 1240 cm⁻¹. **K** was characterized more deeply by ¹H NMR according to Ref R7.

¹H NMR (CD₃CN, 300 MHz): 8.05 (m, 2H), 7.66 (m, 1H), 7.54 (m, 2H), 7.33 (m, 2H), 7.00 (m, 3H), 5.31 (s, 2H).

This above-mentioned procedure was repeated several times at different scales affording yields of **K** of *c.a.* 80%.

12. HPLC analysis and calibration curves ($\lambda = 220$ nm)

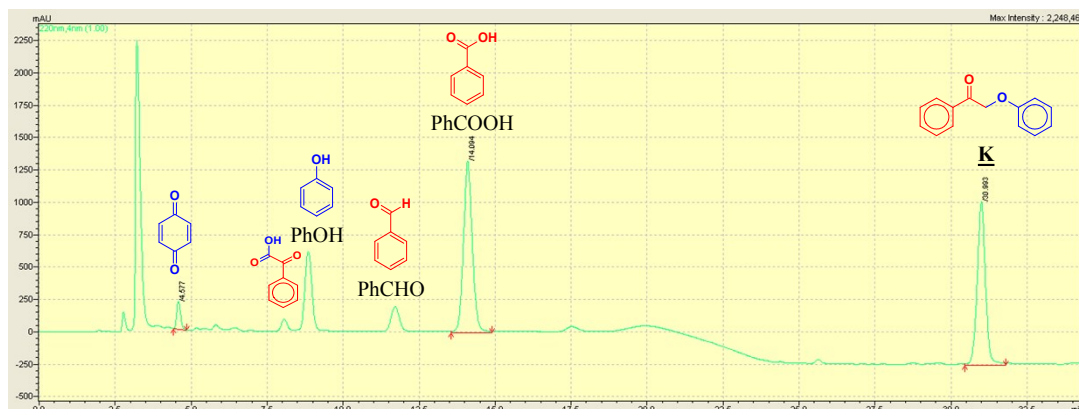
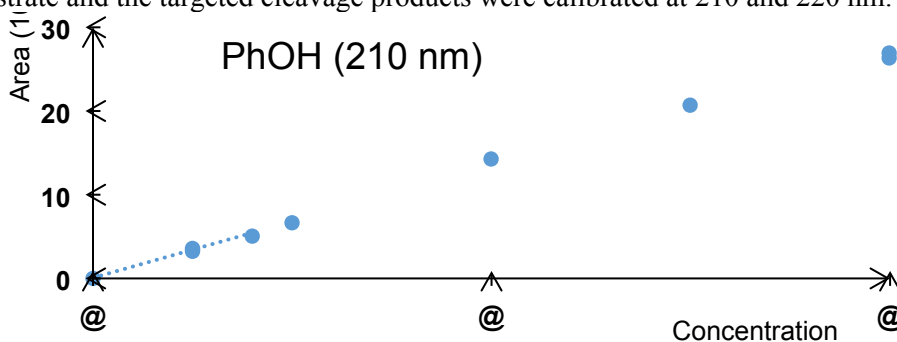


Figure S9. Chromatogram of the reaction mixture for **K** cleavage in the presence of *V*₃-*BM*₅₀-*I*_{BM}-*I*_{5HT} (Conditions detailed in the experimental section of the manuscript and in Table 4, entry 2)

The substrate and the targeted cleavage products were calibrated at 210 and 220 nm.



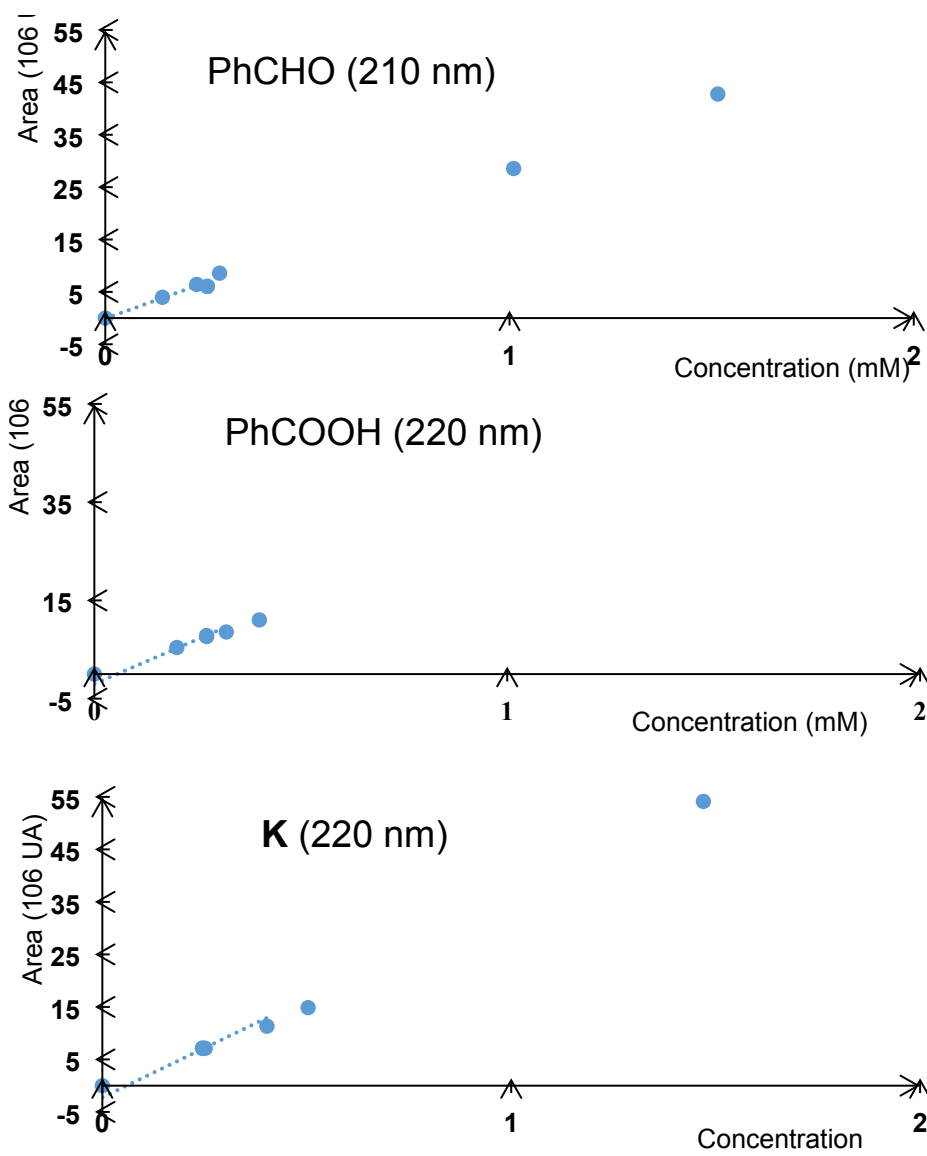


Figure S10. HPLC calibration curves of the products and reactants
(Conditions detailed in the experimental section of the manuscript)

13. References

- [R1] D. Barats-Damatov, L. J. W. Shimon, Y. Feldman, T. Bendikov, R. Neumann, Solid-State Crystal-to-Crystal Phase Transitions and Reversible Structure-Temperature Behavior of Phosphovanadomolybdic Acid, $H_5PV_2Mo_{10}O_{40}$, *Inorg. Chem.* **2015**, 54, 628-634.
- [R2] T. Okuhara, N. Mizuno, M. Misono, Catalytic Chemistry of Heteropoly Compounds, *Adv. Catal.* **1996**, 41, 113-252.
- [R3] P. Villabrille, G. Romanelli, L. Gassa, P. Vázquez, C. Cáceres, Synthesis and characterization of Fe- and Cu-doped molybdovanadophosphoric acids and their application in catalytic oxidation, *Appl. Catal. A: Gen.* **2007**, 324, 69-76.
- [R4] R. Neumann, A. M. Khenkin, Molecular oxygen and oxidation catalysis by

phosphovanadomolybdates, *Chem. Commun.* **2006**, 2529-2538.

[R5] L. Pettersson, Equilibria of Polyoxometalates in Aqueous Solution, *Mol. Eng.* **1993**, 3, 29-42.

[R6] L. Hao, Y. Lu, H. Sato, H. Asanuma, J. Luo, Analysis on energy transfer during mechanical coating and ball milling-Supported by electric power measurement in planetary ball mill, *Intern. J. Mineral Process.* **2013**, 121, 51-58.

[R7] J. M. Nichols, L. M. Bishop, R. G. Bergman, J. A. Ellman, Catalytic C-O Bond Cleavage of 2-Aryloxy-1-arylethanol and Its Application to the Depolymerization of Lignin-Related Polymers, *J. Am. Chem. Soc.* **2010**, 132, 12554-12555.